Chemoproteomic Profiling Identifies Changes in DNA-PK as Markers of Early Dengue Virus Infection

Michael L. Vetter[1], **Mary A. Rodgers**[1,3], **Matthew P. Patricelli**[2], and **Priscilla L. Yang**[1,*]

[1]Department of Microbiology and Immunobiology, Harvard Medical School, Boston, MA, 02115

[2]ActivX Biosciences Inc., La Jolla, CA 92037

Abstract

Many cellular factors are regulated via mechanisms affecting protein conformation, localization, and function that may be undetected by most commonly used RNA- and protein-based profiling methods that monitor steady-state gene expression. Mass spectrometry-based chemoproteomic profiling provides alternatives for interrogating changes in the functional properties of proteins that occur in response to biological stimuli, such as viral infection. Taking dengue virus 2 (DV2) infection as a model system, we utilized reactive ATP- and ADP-acyl phosphates as chemical proteomic probes to detect changes in host kinase function that occur within the first hour of infection. The DNA-dependent protein kinase (DNA-PK) was discovered as a host enzyme with significantly elevated probe labeling within one hour of DV2 infection. Increased probe labeling was associated with increased DNA-PK activity in nuclear lysates and localization of DNA-PK in nucleoli. These effects on DNA-PK were found to require a post-fusion step of DV2 entry and were recapitulated by transfection of cells with RNA corresponding to stem loop B of the DV2 5′ untranslated region. Upon investigation of the potential downstream consequences of these phenomena, we detected a modest but significant reduction in the interferon response induced by DV2 in cells partially depleted of the Ku80 subunit of DNA-PK. These findings identify changes in DNA-PK localization and activity as very early markers of DV2 infection. More broadly, these results highlight the utility of chemoproteomic profiling as a tool to detect changes in protein function associated with different cell states and that may occur on very short time scales.

INTRODUCTION

Detecting functional changes in cellular proteins is challenging given the rapid rate at which these changes can occur. Monitoring changes in steady-state mRNA or protein abundance can provide significant and valuable information on differences in cellular state mediated by changes in steady-state gene expression following specific stimuli but may not detect perturbations of host protein localization, conformation, or activity that can occur on much shorter time scales (*i.e.*, minutes instead of hours). Viral infection is one such stimulus that can cause global changes in steady-state gene expression but can also perturb host protein function and/or localization via mechanisms that are independent of changes in steady-state gene expression.

Kinases, which transduce signals through specific phosphorylation of their substrates, are known to be tightly regulated at multiple levels including transcription, translation, protein stability, and post-translational processes that control structural conformation, localization and protein-protein interactions (1). Given the centrality of kinases in signal transduction and regulation of cellular processes, it is not surprising that viruses are known to exploit host kinases to support their own replication while also targeting cellular kinases to counteract the host response to infection (2-5). Since most virus-induced effects on host kinases have been observed after viral protein expression and replication are well-established, we were interested in using chemoproteomic methods to monitor changes in kinase activity, conformation, localization, or other functional characteristics that might occur on a more rapid timescale early in infection.

KiNativ profiling using ATP- and ADP-acyl phosphate probes has recently been validated as a tool to interrogate changes in kinase function (6, 7). These probes mimic the ATP cofactor but contain an acyl anhydride that reacts with the conserved catalytic lysine and with lysines in the kinase activation loop and other sites proximal to the ATP-binding site. Reaction with these probes results in covalent attachment of the kinase to biotin, which can then be used as an affinity handle to both purify and quantify the extent of labeling via mass spectrometry (Figure 1A). Since the efficiency of probe labeling reflects the binding affinity of the kinase for the probe and its rate of reaction with lysines, quantification of differences in probe-labeling can provide a sensitive measure of changes in functionally relevant properties of kinases, including those due to changes in kinase abundance, post-translational modifications, altered cellular localization, and association with regulatory factors (6-9). While profiling with ATP- and ADP-acyl phosphate probes has primarily been used to profile kinase inhibitor selectivity (7-9), we were interested in demonstrating that these probes can also be useful tools to identify changes in cell state following a specific biological stimulus, such as viral infection. In particular, we were interested in identifying changes that might not be detected using conventional expression-based profiling methods. Using dengue virus as a model system, we undertook experiments to interrogate changes in the functional host kinome that occur very early in viral infection.

Dengue virus (DV) is a single-stranded positive-sense RNA virus comprised by four circulating serotypes (DV1-DV4), which are the causative agent of dengue fever, dengue hemorrhagic fever, and dengue shock syndrome. Although 2.5 billion people living in endemic areas are at risk of infection and an estimated 50-100 million infections per year, there are no DV-specific therapeutics and no available vaccine. DV infection is initiated by clathrin-mediated uptake of the virion following binding to a receptor on the host cell surface. Endosomal acidification triggers conformational changes in the viral envelope protein (E) that catalyze fusion of the viral and endosomal membranes (10). Following release of the viral nucleocapsid into the cytoplasm, the DV genomic RNA is translated to yield a polyprotein that is subsequently cleaved into three structural and seven non-structural proteins. The viral genomic RNA is encapsidated by a shell comprised by core protein, and the assembled nucleocapsid then buds into the ER lumen. As these enveloped viral particles traffic through the secretory pathway of the host cell, they undergo posttranslational processing of the E and prM proteins on the virion surface, ultimately producing mature virions that are secreted from the host cell. Altogether this process occurs on the timescale of several hours with the release of progeny viral particles commencing at 12 to 24 hours post-infection, depending upon the virus strain and cell-type (11, 12). As with many other viruses, cellular kinases that function as effectors of DV replication (13-16) and as effectors of the host innate immune response to DV (17, 18) have been identified through RNAi and small molecule screens as well as transcriptomic and proteomic profiling studies.

To examine whether DV causes detectable changes in the host kinome very early in infection, we performed a chemoproteomic profiling study utilizing KiNativ ATP- and ADP-acyl phosphate probes and a serotype 2 strain of DV (DV2) (Figure 1). This profiling identified DNA-dependent protein kinase (DNA-PK) as a host kinase that exhibits increased labeling within one hour of DV2 infection. Increased labeling of DNA-PK's Ku70, Ku80, and DNA-PKcs subunits was associated with an increase in kinase activity in nuclear lysates from DV2-infected cells and accumulation of DNA-PK in nucleoli. These effects on DNA-PK were recapitulated upon transfection of cells with an *in vitro* synthesized RNA corresponding to stem loop B of the 5′ untranslated region (UTR) of the DV2 genome. RNAi targeting the Ku80 subunit of DNA-PK led to a decrease in DV2-induced interferon expression and signaling. Taken together, our results suggest that DV2's perturbation of DNA-PK activity and localization are very early markers of DV infection and illustrate the utility of this chemoproteomic method to identify differences in kinase function and localization that are associated with changes in cell state.

RESULTS AND DISCUSSION

Chemoproteomic Profiling Identifies Changes in the Host Kinome at an Early Time Point in DV2 Infection

To examine the use of ATP- and ADP-acyl phosphate probes as tools to identify changes in the functional kinome that occur early following a biological stimulus, we profiled the changes induced by DV2 at one hour post-infection. Huh7 cells were infected with DV2 or vesicular stomatitis virus (VSV) at a multiplicity of infection (MOI) of 10, or mock-infected with conditioned medium. VSV, an enveloped, negative-sense RNA virus, was chosen as a control for viral specificity because it replicates rapidly -- progeny virions first appear four hours post-infection (19) -- and because its replication is known to have a significant effect on multiple cellular processes including translation (20) and the interferon response (21). Comparison of the DV2-infected sample to the controls from multiple replicate profiling experiments enabled the discovery that DNA-dependent protein kinase (DNA-PK) is consistently elevated in DV2 samples by two- to eight-fold (Figure 2A). DNA-PK is a heterotrimeric kinase responsible for recognition and repair of DNA double-stranded breaks. The DNA-PKcs subunit contains the kinase active site while Ku70 and Ku80 subunits regulate the catalytic activity of DNA-PKcs, mediate interactions with other proteins, and can act as ATP-dependent helicases (22). All three subunits have conserved lysines near their respective ATP-binding sites, and all three subunits exhibited significantly higher labeling with KiNativ probes in the DV2-infected samples versus VSV-infected or mock-infected controls (Supplementary Tables 1 and 2). Increased labeling of the DV2 samples was confirmed by independent affinity purification of the labeling reactions followed by Western blot analysis for Ku80 (Figure 2B); moreover, Western blot analysis of the unlabeled lysate confirmed that this result was not due to increased steady-state expression of Ku70 or Ku80 (Figure 2C).

Both the DV2- and VSV-infected samples also exhibited moderate changes in additional kinases that were at or below our set level of significance (Supplementary Table 1). These kinases may still reflect physiologically important DV2-host interactions since even modest changes in enzyme conformation and activity can have significant effects on downstream kinase targets and the processes they regulate. We also note that although the ATP-/ADP-acyl phosphate probes utilized in this study were developed as tools for functional interrogation of the kinome (7), our finding that Ku70 and Ku80 also exhibited increased labeling with these probes illustrates their potential as tools to monitor changes in other nucleotide-binding proteins.

Increased chemoproteomic labeling of DNA-PK is correlated with changes in kinase function and localization in DV2-infected cells

To investigate whether increased labeling with KiNativ probes corresponded to a detectable change in kinase function, we examined the effects of DV2 on kinase activity and localization at 60 minutes post-infection. Nuclear lysates prepared from DV2-infected cells were analyzed using a commercially available $[\gamma\text{-}^{32}P]$ATP-based DNA-PK activity assay and found to have elevated DNA-PK enzymatic activity compared to mock-infected and VSV-infected controls (Figure 2D). We also monitored the localization of the Ku70 subunit as a marker of DNA-PK at 10, 30, and 60 minutes post-DV2 infection by immunofluorescence microscopy. Ku70 localized to specific sites in the nucleus by 60 minutes post-DV2 infection (Supplementary Figure 1A), and co-localization with nucleolin confirmed that these compartments were nucleoli (Figure 3A). This effect was not limited to Ku70, since Ku80 and DNA-PKcs exhibited nucleolar localization at one hour post-DV2 infection (Supplementary Figure 1B). Importantly, cells infected with VSV or exposed to conditioned medium for one hour did not exhibit accumulation of DNA-PK subunits in the nucleoli (Figure 3B and Supplementary Figure 1B). Nucleolar DNA-PK was also not observed following infection of cells with Kunjin virus (MOI 10), a member of the *Flaviviridae* family that is closely related to DV2 (Figure 3C). Together these data indicate that DNA-PK activity and localization undergo changes very early in DV2 infection and that these perturbations are specific to DV2 versus being part of a generic antiviral or stress response. More broadly, these results illustrate the utility of the ATP-/ADP-acyl phosphate probes in discovering virus-induced changes in host protein function and localization very early in viral infection.

Early Events in DV2 Infection Trigger Nucleolar Localization of DNA-PK

Based on the relatively rapid kinetics of DV2's effects on DNA-PK activity and localization, we hypothesized that these events might be triggered during DV2 entry – known to have an average time between surface binding and endosomal fusion of 12.5 minutes (23, 24) -- or shortly thereafter. To test this hypothesis, we first asked whether DV2-induced changes in DNA-PK localization occur in the presence of chloroquine, a compound that inhibits DV2 entry by blocking endosomal acidification. Using immunofluorescence detection of Ku70 as a marker for the localization of the heterotrimeric DNA-PK complex, we found that DNA-PK localization is unchanged at 60 minutes post-DV2 infection in the presence of this compound (Supplementary Figure 1C). Since blocking endosomal acidification might affect DNA-PK localization via mechanisms unrelated to DV2 entry, we also utilized a peptide derived from the DV2 E protein stem region (the "DV2 stem peptide") that specifically inhibits the fusion step of DV entry (25, 26). In the presence of the DV2 stem peptide, Ku70 remained nuclear and did not accumulate in nucleoli at 60 minutes post-DV2 infection (Figure 4A). These data suggested that viral-endosomal membrane fusion or a downstream event, such as nucleocapsid escape to the cytoplasm, is necessary to trigger nucleolar localization of DNA-PK.

To test whether viral-endosomal membrane fusion is sufficient to cause nucleolar localization of DNA-PK, we utilized virus-like particles (VLPs), which contain only the prM/M and E proteins embedded in a viral membrane and which lack the viral nucleocapsid (27). Since DV2 VLPs have mature E protein (27), their entry into cells is believed to occur via the same processes of attachment, clathrin-mediated endocytosis, and membrane fusion mediated by E on the surface of authentic virions. Incubation of Huh7 cells with 0.5 μg VLPs -- equivalent in mass to the DV2 virions used in this set of experiments --had no effect on Ku70 localization at 60-minutes post-infection (Figure 4B). This suggested that viral-endosomal membrane fusion is not sufficient to perturb DNA-PK localization and that this

phenomenon occurs only upon postfusion events that are not recapitulated by the VLP system.

Transfection of DV2 5′ UTR RNAs Causes Re-localization of DNA-PK to the Nucleoli

Since expression of new viral gene products is usually detected 8 - 12 hours post-DV infection (28, 29), the effects of DV2 on DNA-PK at 60 minutes post-infection seemed more likely triggered by the incoming DV2 genomic RNA and/or core protein, both of which are present in the virion but absent from the VLP. Recognition of viral nucleic acids by host pattern recognition receptors (PRRs) initiates the innate immune response, and *in vitro* transcribed RNAs corresponding to the 5′ and 3′ untranslated regions (UTRs) of the DV2 genome (Figure 5) are moderate activators of the interferon response when transfected directly into cells (30). To examine whether DV2's effects on DNA-PK can be triggered by the 5′ or 3′ UTRs, we transfected cells with the corresponding *in vitro* synthesized transcripts and monitored the effect on Ku70 localization at 60 minutes post-transfection. As illustrated in Figure 5C, transfection of Huh7 cells with a capped 5′ UTR RNA was associated with nucleolar Ku70 that resembled DNA-PK's localization following DV2 infection (Figure 3). This did not appear to be a generic effect of the RNA transfection since neither the lipid transfection reagent alone nor transfection of the 3′ UTR RNA were associated with nucleolar Ku70. In addition, the effect of the 5′ UTR RNA was not due to the adenosine cap since transfection of cells with a non-capped 5′ UTR RNA also resulted in nucleolar DNA-PK (Supplementary Figure 1D).

To map the region of the 5′ UTR RNA sufficient to affect Ku70 localization, we examined the effects of equivalent masses of *in vitro* synthesized RNAs corresponding to conserved stem loops A and B (Figure 5B), whose secondary structures have been verified by chemical and nuclease mapping in solution (31). Transfection of stem loop B RNA but not stem loop A RNA was associated with a change in Ku70 localization (Figure 5D) that recapitulated the effects of both the 5′ UTR RNA transfection (Figure 5C) and infection with authentic DV2 (Figures 3 and 4). In addition, transfection of Huh7 cells with stem loop B RNA was correlated with an increase in DNA-PK kinase activity in nuclear lysates generated at 60 minutes post-transfection, whereas stem loop A and the 5′ UTR RNAs caused no measurable change in DNA-PK activity in these experiments (Figure 5E). Taken together these results demonstrate that stem loop B alone is sufficient to affect both the activity and localization of DNA-PK.

The secondary structure of the 5′ UTR is well conserved among the four DV serotypes and has been implicated in interactions with host factors as well as in the regulation of both translation and replication of the viral genomic RNA (32-34). While the 5′ UTR secondary structure, including stem loop B, is fairly conserved across the *Flaviviridae*, the failure of Kunjin virus infection to trigger changes in DNA-PK localization (Figure 3C), indicates that further work is needed to elucidate the molecular features of the DV2 stem loop B RNA that are responsible for triggering its effects on DNA-PK. Interestingly, although the stem loop B RNA affected both DNA-PK activity and localization, these two perturbations appeared to be uncoupled in the experiments utilizing the 5′ UTR RNA (Figure 5C and 5E). In addition, the nucleolar localization of DNA-PK following DV2 infection or transfection with stem loop B RNA was unaffected by the presence of 10 µM NU7114 (35), a small molecule inhibitor of DNA-PK, (Supplementary Figure 2), suggesting that the kinase activity is not required for the DV2-induced change in localization. While these results could suggest that these phenomena are functionally and mechanistically distinct, further study is required to elucidate their functional significance and the mechanisms responsible.

RNAi-mediated Depletion of Ku80 Perturbs Activation of the Host Interferon Response

Since DNA-PK has previously been implicated in signal transduction regulating the interferon response (36, 37), we sought to test the effect of RNAi-mediated depletion of DNA-PK subunits on DV2 replication and the host interferon response to DV2 infection (Figure 6A). Huh7 cells were transfected with siRNA pools targeting Ku70 and/or Ku80 or with a non-targeting siRNA control, and then 48 hours later were infected with DV2 (MOI 1). At 24 hours post-infection, the yield of infectious virus in the culture supernatants was titered by focus forming assay. Consistent with previous reports (38), we observed that RNAi-targeting one DNA-PK subunit resulted in simultaneous depletion of the other subunit (Figure 6B). Interestingly, the yield of DV2 progeny virions at 24 hours post-infection appeared unaffected by RNAi targeting Ku70 and/or Ku80 (Figure 6C), suggesting that DNA-PK is not required for DV2 replication although we cannot exclude the possibility that the partial depletion of Ku70 and Ku80 in our experiments -- 50% and 40%, respectively, by Western blot -- was insufficient to cause a measurable DV2 phenotype by this assay. Next, we examined the effect of RNAi-mediated depletion of DNA-PK subunits on DV2-induced interferon expression and signaling by quantifying IFN-β mRNA copy number and by using reporter plasmids in which firefly luciferase expression is regulated by the IFN-beta or interferon-sensitive response element (ISRE) promoters. RNAi-mediated depletion of Ku80 but not Ku70 was associated with a modest decrease in IFN-β mRNA (Figure 6D) as well as decreases in IFN and ISRE promoter activity following DV2 infection (Figures 6E and 6F). We note that since there is considerable redundancy amongst the mechanisms that activate and regulate the interferon response to viral infection, a very early contribution to this response by DNA-PK might be somewhat obscured by downstream effectors that are amplified upon new gene expression and that activate, potentiate, or dampen this response (39). Taken in this light, even the modest effects that we observed may be functionally significant, particularly since they were observed with only partial depletion of Ku80.

Although DNA-PK has been implicated in the life cycles of adenovirus (40) and HIV (41), it has not previously been identified in genome-wide RNAi screens designed to identify host factors required for productive replication of DV or related flaviviruses (15, 42). In this study, we observed that partial depletion of Ku70 and/or Ku80 by RNAi had no effect on the replication of DV2 (Figure 6C), findings that are consistent with a model in which DNA-PK is part of the host cell's early detection of DV2 rather than a host factor exploited to enhance viral replication. While additional studies are required to elucidate the biological function(s) of DNA-PK in the host response to dengue virus, our findings demonstrate that changes in DNA-PK activity and localization appear to be very early, specific markers of DV infection.

Potential role of DNA-PK as a signal transducer in the response to cellular stresses, including DV2 infection

Consistent with its function, increases in DNA-PK activity have been directly correlated with localization of the protein to the site of DNA double-stranded breaks in the nucleus (43); however, DNA-PK has also been reported to localize in cytoplasmic lipid rafts and the plasma membrane (44). Since the nucleoli are physically separated from the site of incoming DV2 in our experiments, we deem it unlikely that nucleolar DNA-PK interacts directly with the DV2 RNA. Instead, DV2 may interact with cytoplasmic DNA-PK prior to its translocation to nucleoli or DNA-PK may lie downstream of signaling events triggered upon release of the DV2 RNA in the cytoplasm and detection of DV2 RNA by cytosolic RNA sensors. Notably, nucleolar localization of DNA-PK in a manner dependent on the cell cycle or stress status of the cell has been observed (43, 45), and DNA-PK activity is known to be modulated by cellular stress conditions such as hypoxia (46) and ionizing radiation (44). Additional experiments are needed to determine the relationship between these pathways and the changes in DNA-PK activity and localization associated with DV2 infection.

Importantly, since RNAi against Ku80 and Ku70 had differing effects on the DV2-stimulated interferon response (Figure 6), the function(s) of individual DNA-PK subunits in the host interferon response remain to be elucidated.

Significance

In conclusion, this study illustrates the utility of chemoproteomic profiling with ATP-/ADP-acyl phosphate probes to identify specific changes in the host kinome that would likely not be detected using conventional approaches that measure changes in host mRNA or protein abundance. Importantly, this analysis permitted the discovery that changes in DNA-PK localization and activity are early, specific markers of DV2 infection. Our results provide the basis for future studies to determine whether the DV2-induced perturbations of DNA-PK are also functionally important in DV2 replication and/or the host response to DV2. In addition, our results suggest that chemical proteomic profiling methods using ATP-/ADP-acyl phosphate probes and other probes of host protein function will be a broadly useful strategy not only in interrogating pathogen-induced changes in host cell signaling, but also more broadly in identifying changes in kinase function and localization associated with different cell states. This is an important development because the majority of '-omic' approaches have focused on measuring changes in steady-state DNA, RNA and protein while biochemically based '-omic' approaches interrogating protein function have been under-developed.

METHODS

Additional experimental details are provided in Supporting Information online.

Cells and viruses

Human hepatoma (Huh7) cells and HEK 293T cells were maintained in DMEM supplemented with 10% fetal bovine serum. DV2 New Guinea strain C (NGC) was grown in C6/36 mosquito cells maintained in L-15 medium supplemented with 10% (v/v) FBS. Dengue virions were purified (26) and titered by focus-forming assay (FFU) (47).

Chemoproteomic profiling with biotinylated ATP-/ADP-acyl phosphate probes

Profiling experiments were performed as previously described (6, 7). 8×10^7 cells Huh7 cells were incubated with conditioned media or infected with DV2 or VSV (MOI 10). At sixty minutes of infection, cells were washed with PBS and lifted from the culture flask by Versene (Invitrogen). Cells were pelleted, resuspended in buffer A (25 mM Tris pH 7.6, 150 mM NaCl, 1 % (v/v) CHAPS, 1% (v/v) Tergitol and phosphatase inhibitor cocktail II (EMD)) equal to 4 times the pelleted cell volume, and then Dounce homogenized and sonicated. Debris was pelleted by centrifugation (13000 X g, 4 °C, 30 min) followed by buffer exchange of supernatant to buffer B (20 mM HEPES, 150 mM NaCl, 0.1% (v/v) Triton X-100, phosphatase inhibitor cocktail II (EMD)) via BioRad 10DG column. Protein concentrations were determined by the DC Protein Assay (BioRad). 0.5 mL lysate at a total concentration of 3 mg ml^{-1} was incubated in the presence of 5 μM ATP- or ADP-acyl phosphate probe for 10 minutes at 25 °C. Proteins were denatured by addition of 0.5 mL 12 M Urea, reduced with DTT (10 mM), and then reacted with 40 mM iodoacetamide to block cysteine thiols. Following size exclusion chromatography to remove excess reagents, the reactions were digested with trypsin. Probe-labeled peptides were captured with streptavidin-agarose beads (Pierce), washed, and eluted in a 50% acetonitrile/water mixture with 0.1% TFA. *Mass Spectrometry Analysis-* Samples were analyzed by LC-MS/MS on Finnigan LCQ Deca XP ion trap mass spectrometers as described previously (48, 49). Data were searched using the Sequest algorithm with searching and scoring modifications described previously (48, 49). A modification mass of 196.2 Da was used as a variable

modification on lysine for search purposes. Two samples for each experimental condition were labeled and analyzed. Observed fold changes greater than +/− 1.5 relative to the conditioned media were considered significant if they were at least 2 times greater than the standard deviation of the 4 possible comparisons to be made (conditioned medium sample 1 vs. DV2 sample 1, conditioned medium sample 2 vs. DV2 sample 1, conditioned medium sample 1 vs. DV2 sample 2, and conditioned medium sample 2 vs. DV2 sample 2). The profiling experiments were performed a total of four times with 2 replicates of each experimental condition per profiling experiment.. To confirm increased probe-labeling, labeling reactions were processed using the Pierce Kinase Enrichment Kit (Thermo Scientific) according to the manufacturer's instructions prior to analysis of the labeled products by Western blot.

Ku70/80 Western Blot

Cells were lysed in RIPA buffer (Boston Bioproducts) supplemented with protease inhibitors (Roche). Lysates were separated by SDS-PAGE and then transferred to nitrocellulose membrane. Membranes were blocked and then stained using primary antibodies against Ku80 and Ku70 as described in SI Materials and Methods.

DNA-PK activity assay

Following preparation of nuclear extracts (50), a commercial DNA-PK activity assay (Promega) was performed following the manufacturer's instructions and quantified using a storage phosphor imaging system (Typhoon and Image Quant TL).

VLP production and purification

The plasmid encoding a mammalian codon-optimized DV2 prM-E expression cassette was generously provided by S. Harrison. VLPs were prepared in HEK293T cells and purified as previously described (47).

Immunofluorescence Confocal Microscopy

Cells were fixed, blocked in 1% (w/v) BSA/PBS, and then stained using primary antibodies against Ku70 (Abcam), Ku80 (Cell Signaling Technology), DNA-PKcs (Abcam), or nucleolin (Sigma) and the appropriate anti-mouse IgG1-FITC (Life Technologies), anti-rabbit Texas Red (Jackson Immunoresearch), anti-rabbit Alexa Fluor 647 (Life Technologies), and anti-mouse IgG1-FITC, respectively. Images were acquired using a QuantEM (Photometrics) cooled charge-coupled device as part of a CSU-X1 spinning disk confocal system (Yokogawa Electric Corporation). Initial data capture was performed using Slidebook software (Intelligent Imaging Innovations). Further processing was performed using Metamorph (Molecular Devices). Each figure represents a single plane from the Z-stack.

In Vitro Transcription and Transfection of DV2 RNAs

cDNAs encoding the 5′UTR, 3′UTR, and stem loop A RNAs were PCR-amplified from pRS-DEN2, which contains the complete DV2 New Guinea C genome, using primers that contained the T7 promoter sequence. cDNA encoding stem loop B was produced by annealing of synthetic DNA oligos. *In vitro* transcription reactions were performed with Ampliscribe™ T7 (Cellscript), and RNA transfections using Lipofectamine (Invitrogen) were performed using 3 µg of the appropriate RNA following the manufacturers' instructions.

RNAi analysis

Huh7 cells were reverse transfected with MISSION siRNA pools and infected with DV2 (MOI 1) at 48 hours post-transfection. For promoter assays, cells were transfected with a plasmid encoding firefly luciferase under the control of the interferon-beta or ISRE promoters along with plasmid pRL-CMV encoding renilla luciferase as a transfection control at 24 hours post-siRNA transfection followed by infection with DV2 24 hours later. At 24 hours post-infection, the yield of infectious DV2 in culture supernatants was measured by FFA while GAPDH and IFN-beta RNA were quantified by qRT-PCR assay using the iQ SYBR Green Supermix (Biorad) and primers specific for IFN-β and GAPDH and dual luciferase assays were performed using a commercially available kit (Promega).

Supplementary Material

Refer to Web version on PubMed Central for supplementary material.

Acknowledgments

REFERENCES

1. Huse M, Kuriyan J. The conformational plasticity of protein kinases. Cell. 2002; 109:275–282. [PubMed: 12015977]

2. Fujioka Y, Tsuda M, Hattori T, Sasaki J, Sasaki T, Miyazaki T, Ohba Y. The Ras-PI3K signaling pathway is involved in clathrin-independent endocytosis and the internalization of influenza viruses. PLoS One. 2011; 6:e16324. [PubMed: 21283725]

3. Li E, Stupack DG, Brown SL, Klemke R, Schlaepfer DD, Nemerow GR. Association of p130CAS with phosphatidylinositol-3-OH kinase mediates adenovirus cell entry. J Biol Chem. 2000; 275:14729–1. [PubMed: 10799562]

4. Dauber B, Wolff T. Activation of the Antiviral Kinase PKR and Viral Countermeasures. Viruses. 2009; 1:523–544. [PubMed: 21994559]

5. Dunn EF, Connor JH. HijAkt: The PI3K/Akt pathway in virus replication and pathogenesis. Prog Mol Biol Transl Sci. 2012; 106:223–250. [PubMed: 22340720]

6. Patricelli MP, Nomanbhoy TK, Wu J, Brown H, Zhou D, Zhang J, Jagannathan S, Aban A, Okerberg E, Herring C, Nordin B, Weissig H, Yang Q, Lee JD, Gray NS, Kozarich JW. In situ kinase profiling reveals functionally relevant properties of native kinases. Chem Biol. 2011; 18:699–710. [PubMed: 21700206]

7. Patricelli MP, Szardenings AK, Liyanage M, Nomanbhoy TK, Wu M, Weissig H, Aban A, Chun D, Tanner S, Kozarich JW. Functional interrogation of the kinome using nucleotide acyl phosphates. Biochemistry. 2007; 46:350–358. [PubMed: 17209545]

8. Deng X, Dzamko N, Prescott A, Davies P, Liu Q, Yang Q, Lee JD, Patricelli MP, Nomanbhoy TK, Alessi DR, Gray NS. Characterization of a selective inhibitor of the Parkinson's disease kinase LRRK2. Nat Chem Biol. 2011; 7:203–205. [PubMed: 21378983]

9. Liu Q, Kirubakaran S, Hur W, Niepel M, Westover K, Thoreen CC, Wang J, Ni J, Patricelli MP, Vogel K, Riddle S, Waller DL, Traynor R, Sanda T, Zhao Z, Kang SA, Zhao J, Look AT, Sorger PK, Sabatini DM, Gray NS. Kinome-wide selectivity profiling of ATP-competitive mammalian target of rapamycin (mTOR) inhibitors and characterization of their binding kinetics. J Biol Chem. 2012; 287:9742–9752. [PubMed: 22223645]

10. Stiasny K, Fritz R, Pangerl K, Heinz FX. Molecular mechanisms of flavivirus membrane fusion. Amino Acids. 2011; 41:1159–1163. [PubMed: 19882217]

11. Chambers TJ, Hahn CS, Galler R, Rice CM. Flavivirus genome organization, expression, and replication. Ann Rev Microbiol. 1990; 44:649–688. [PubMed: 2174669]

12. Fink J, Gu F, Ling L, Tolfvenstam T, Olfat F, Chin KC, Aw P, George J, Kuznetsov VA, Schreiber M, Vasudevan SG, Hibberd ML. Host gene expression profiling of dengue virus infection in cell lines and patients. PLoS Negl Trop Dis. 2007; 1:e86. [PubMed: 18060089]

13. Chu JJ, Yang PL. c-Src protein kinase inhibitors block assembly and maturation of dengue virus. Proc Natl Acad Sci U S A. 2007; 104:3520–3525. [PubMed: 17360676]

14. Bhattacharya D, Mayuri, Best SM, Perera R, Kuhn RJ, Striker R. Protein kinase G phosphorylates mosquito-borne flavivirus NS5. J Virol. 2009; 83:9195–9205. [PubMed: 19587048]

15. Sessions OM, Barrows NJ, Souza-Neto JA, Robinson TJ, Hershey CL, Rodgers MA, Ramirez JL, Dimopoulos G, Yang PL, Pearson JL, Garcia-Blanco MA. Discovery of insect and human dengue virus host factors. Nature. 2009; 458:1047–1050. [PubMed: 19396146]

16. Colpitts TM, Cox J, Vanlandingham DL, Feitosa FM, Cheng G, Kurscheid S, Wang P, Krishnan MN, Higgs S, Fikrig E. Alterations in the Aedes aegypti transcriptome during infection with West Nile, dengue and yellow fever viruses. PLoS Pathog. 2011; 7:e1002189. [PubMed: 21909258]

17. Jiang D, Weidner JM, Qing M, Pan XB, Guo H, Xu C, Zhang X, Birk A, Chang J, Shi PY, Block TM, Guo JT. Identification of five interferon-induced cellular proteins that inhibit west nile virus and dengue virus infections. J Virol. 2010; 84:8332–8341. [PubMed: 20534863]

18. Ceballos-Olvera I, Chavez-Salinas S, Medina F, Ludert JE, del Angel RM. JNK phosphorylation, induced during dengue virus infection, is important for viral infection and requires the presence of cholesterol. Virology. 2010; 396:30–36. [PubMed: 19897220]

19. Timm A, Yin J. Kinetics of virus production from single cells. Virology. 2012; 424:11–17. [PubMed: 22222212]

20. Barber GN. VSV-tumor selective replication and protein translation. Oncogene. 2005; 24:7710–7719. [PubMed: 16299531]

21. Rieder M, Conzelmann KK. Rhabdovirus evasion of the interferon system. Journal of Interferon & Cytokine Research. 2009; 29:499–509. [PubMed: 19715459]

22. Collis SJ, DeWeese TL, Jeggo PA, Parker AR. The life and death of DNA-PK. Oncogene. 2005; 24:949–961. [PubMed: 15592499]

23. van der Schaar HM, Rust MJ, Waarts BL, van der Ende-Metselaar H, Kuhn RJ, Wilschut J, Zhuang X, Smit JM. Characterization of the early events in dengue virus cell entry by biochemical assays and single-virus tracking. J Virol. 2007; 81:12019–12028. [PubMed: 17728239]

24. van der Schaar HM, Rust MJ, Chen C, van der Ende-Metselaar H, Wilschut J, Zhuang X, Smit JM. Dissecting the cell entry pathway of dengue virus by single-particle tracking in living cells. PLoS Pathog. 2008; 4:e1000244. [PubMed: 19096510]

25. Schmidt AG, Yang PL, Harrison SC. Peptide inhibitors of flavivirus entry derived from the E protein stem. J Virol. 2010; 84:12549–12554. [PubMed: 20881042]

26. Schmidt AG, Yang PL, Harrison SC. Peptide inhibitors of dengue-virus entry target a late-stage fusion intermediate. PLoS Pathog. 2010; 6:e1000851. [PubMed: 20386713]

27. Wang PG, Kudelko M, Lo J, Siu LY, Kwok KT, Sachse M, Nicholls JM, Bruzzone R, Altmeyer RM, Nal B. Efficient assembly and secretion of recombinant subviral particles of the four dengue serotypes using native prM and E proteins. PLoS One. 2009; 4:e8325. [PubMed: 20016834]

28. Poungsawai J, Kanlaya R, Pattanakitsakul SN, Thongboonkerd V. Subcellular localizations and time-course expression of dengue envelope and non-structural 1 proteins in human endothelial cells. Microb Pathog. 2011; 51:225–229. [PubMed: 21575706]

29. Pena J, Harris E. Early Dengue Virus Protein Synthesis Induces Extensive Rearrangement of the Endoplasmic Reticulum Independent of the UPR and SREBP-2 Pathway. PLoS One. 2012; 7:e38202. [PubMed: 22675522]

30. Uzri D, Gehrke L. Nucleotide sequences and modifications that determine RIG-I/RNA binding and signaling activities. J Virol. 2009; 83:4174–4184. [PubMed: 19224987]
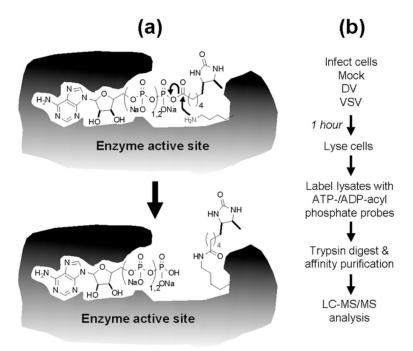
31. Polacek C, Foley JE, Harris E. Conformational changes in the solution structure of the dengue virus 5′ end in the presence and absence of the 3′ untranslated region. J Virol. 2009; 83:1161–1166. [PubMed: 19004957]

32. Alvarez DE, De Lella Ezcurra AL, Fucito S, Gamarnik AV. Role of RNA structures present at the 3′ UTR of dengue virus on translation, RNA synthesis, and viral replication. Virology. 2005; 339:200–212. [PubMed: 16002117]

33. Friebe P, Shi PY, Harris E. The 5′ and 3′ downstream AUG region elements are required for mosquito-borne flavivirus RNA replication. J Virol. 2011; 85:1900–1905. [PubMed: 21123391]

34. Gomila RC, Martin GW, Gehrke L. NF90 binds the dengue virus RNA 3′ terminus and is a positive regulator of dengue virus replication. PLoS One. 2011; 6:e16687. [PubMed: 21386893]

35. Zhao Y, Thomas HD, Batey MA, Cowell IG, Richardson CJ, Griffin RJ, Calvert AH, Newell DR, Smith GC, Curtin NJ. Preclinical evaluation of a potent novel DNA-dependent protein kinase inhibitor NU7441. Cancer Res. 2006; 66:5354–5362. [PubMed: 16707462]

36. Karpova AY, Trost M, Murray JM, Cantley LC, Howley PM. Interferon regulatory factor-3 is an in vivo target of DNA-PK. Proc Natl Acad Sci U S A. 2002; 99:2818–2823. [PubMed: 11867762]

37. Katakura K, Lee J, Rachmilewitz D, Li G, Eckmann L, Raz E. Toll-like receptor 9-induced type I IFN protects mice from experimental colitis. J Clin Invest. 2005; 115:695–702. [PubMed: 15765149]

38. Bertolini LR, Bertolini M, Anderson GB, Maga EA, Madden KR, Murray JD. Transient depletion of Ku70 and Xrcc-by RNAi as a means to manipulate the non-homologous end-joining pathway. J Biotechnol. 2007; 128:246–257. [PubMed: 17097754]

39. Munoz-Jordan JL. Subversion of interferon by dengue virus. Curr Top Microbiol Immunol. 2010; 338:35–44. [PubMed: 19802576]

40. Schwartz RA, Carson CT, Schuberth C, Weitzman MD. Adeno-associated virus replication induces a DNA damage response coordinated by DNA-dependent protein kinase. J Virol. 2009; 83:6269–6278. [PubMed: 19339345]

41. Daniel R, Greger JG, Katz RA, Taganov KD, Wu X, Kappes JC, Skalka AM. Evidence that stable retroviral transduction and cell survival following DNA integration depend on components of the nonhomologous end joining repair pathway. J Virol. 2004; 78:8573–8581. [PubMed: 15280466]

42. Krishnan MN, Ng A, Sukumaran B, Gilfoy FD, Uchil PD, Sultana H, Brass AL, Adametz R, Tsui M, Qian F, Montgomery RR, Lev S, Mason PW, Koski RA, Elledge SJ, Xavier RJ, Agaisse H, Fikrig E. RNA interference screen for human genes associated with West Nile virus infection. Nature. 2008; 455:242–245. [PubMed: 18690214]

43. Dejmek J, Iglehart JD, Lazaro JB. DNA-dependent protein kinase (DNA-PK)-dependent cisplatin-induced loss of nucleolar facilitator of chromatin transcription (FACT) and regulation of cisplatin sensitivity by DNA-PK and FACT. Mol Cancer Res. 2009; 7:581–591. [PubMed: 19372586]

44. Lucero H, Gae D, Taccioli GE. Novel localization of the DNA-PK complex in lipid rafts: a putative role in the signal transduction pathway of the ionizing radiation response. J Biol Chem. 2003; 278:22136–22143. [PubMed: 12672807]

45. Yaneva M, Jhiang S. Expression of the Ku protein during cell proliferation. Biochim Biophys Acta. 1991; 1090:181–187. [PubMed: 1932109]

46. Bouquet F, Ousset M, Biard D, Fallone F, Dauvillier S, Frit P, Salles B, Muller C. A DNA-dependent stress response involving DNA-PK occurs in hypoxic cells and contributes to cellular adaptation to hypoxia. J Cell Sci. 2011; 124:1943–1951. [PubMed: 21576354]

47. de Wispelaere M, Yang PL. Mutagenesis of the DI/DIII Linker in Dengue Virus Envelope Protein Impairs Viral Particle Assembly. J Virol. 2012; 86:7072–7083. [PubMed: 22532681]

48. Adam GC, Burbaum J, Kozarich JW, Patricelli MP, Cravatt BF. Mapping enzyme active sites in complex proteomes. J Am Chem Soc. 2004; 126:1363–1368. [PubMed: 14759193]

49. Okerberg ES, Wu J, Zhang B, Samii B, Blackford K, Winn DT, Shreder KR, Burbaum JJ, Patricelli MP. High-resolution functional proteomics by active-site peptide profiling. Proc Natl Acad Sci U S A. 2005; 102:4996–5001. [PubMed: 15795380]

50. Abmayr SM, Yao T, Parmely T, Workman JL. Preparation of nuclear and cytoplasmic extracts from mammalian cells. Curr Protoc Mol Biol Chapter. 2006; 12 Unit 12 11.

51. Leahy JJ, Golding BT, Griffin RJ, Hardcastle IR, Richardson C, Rigoreau L, Smith GC. Identification of a highly potent and selective DNA-dependent protein kinase (DNA-PK) inhibitor (NU7441) by screening of chromenone libraries. Bioorg Med Chem Lett. 2004; 14:6083–6087. [PubMed: 15546735]

Figure 1. Chemoproteomic Profiling Using ATP- and ADP-Acyl Phosphate Probes
(a) Structures of the KiNativ ATP- and ADP-acyl phosphate probes and their covalent reaction with lysines in or proximal to the ATP binding site of kinases and other enzymes.
(b) Scheme of the chemoproteomic profiling experiment to identify DV2-induced changes in host kinase function.
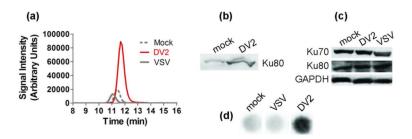
Figure 2. DNA-PK Exhibits Increased Labeling and Catalytic Activity at 60 minutes Post-DV2 Infection
(a) Representative mass spectrometry trace showing the relative intensity of the probe-labeled DNA-PK catalytic subunit peptide in samples prepared from Huh7 cells treated with conditioned medium (Mock) or infected with DV2 (MOI 10) or VSV (MOI 10). Four separate profiling experiments were performed, each time analyzing two replicate samples for each experimental condition. (b) Western blot confirmation of increased reaction of the Ku80 subunit of DNA-PK with the ATP-acyl phosphate probe in DV2-infected lysates versus mock-infected lysates. (c) Representative Western blot of unlabeled protein lysates demonstrating no change in steady-state expression of Ku70 or Ku80 following DV2 infection. (d) Kinase assay confirming that nuclear lysates from DV2-infected cells exhibit increased DNA-PK kinase activity relative to mock-infected and VSV-infected controls. Representative data for three separate experiments are shown. Note that all samples for this radiometric assay were analyzed on the same filter. The intervening space on the filter between the VSV and DV2 samples was eliminated to reduce the size of this image.
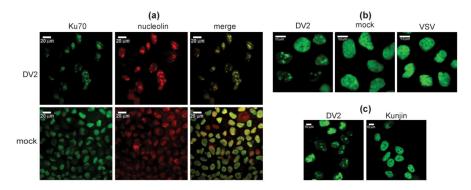
Figure 3. DNA-PK Exhibits Nucleolar Localization Early in DV2 Infection
Huh7 cells were infected with DV2 (MOI 10) and then fixed and analyzed by immunofluorescence microscopy to monitor the localization of **(a)** Ku70, which co-localizes with nucleolin at 60 minutes post-DV2 infection. Neither **(b)** VSV nor **(c)** Kunjin virus infections cause nucleolar localization of Ku70 at this time post-infection. Images are representative of three separate experiments.
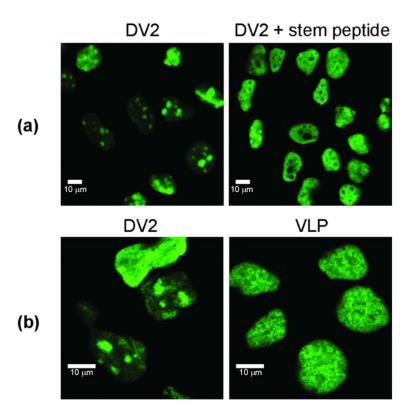
Figure 4. A Post-Fusion Event Is Required to Trigger the DV2-Induced Change in DNA-PK Localization
(a) Inhibition of the fusion step of DV2 entry with the DV2 stem peptide prevents nucleolar localization of Ku70 at 60 minutes post-DV2 infection. **(b)** Incubation of Huh7 cells with purified dengue virions leads to nucleolar Ku70, which is not observed upon incubation of cells with an equivalent mass of VLPs. Images are representative of three separate experiments.
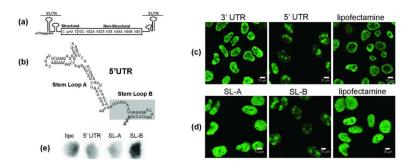
Figure 5. Transfection of the DV2 5′ UTR Stem Loop B RNA Is Sufficient to Cause Changes in DNA-PK Translocation and Enzymatic Activity
(a) Schematic of the DV2 genome indicating the location of the 5′ and 3′ UTRs. (b) Secondary structure of the DV2 5′UTR indicating the locations of stem loops A and B. Stem loop B is shaded in gray with the start codon in bold type and underlined. Adapted from reference 31. (c) At 60 minutes post-transfection, Ku70 localizes in the nucleoli of cells transfected with the 5′ UTR RNA but not of cells treated with transfection reagent alone or cells transfected with the 3′ UTR RNA. (d) Ku70 is observed in the nucleoli of cells transfected with the 5′ UTR and stem loop B (SLB) RNAs but not in cells treated with transfection reagent alone (no RNA) or cells transfected with the stem loop A (SLA) RNA. (e) DNA-PK activity is elevated in nuclear lysates from cells transfected with SLB RNA but not lysates from cells transfected with 5′ UTR or SLA RNAs or treated with transfection reagent alone. Images are representative of three separate experiments.
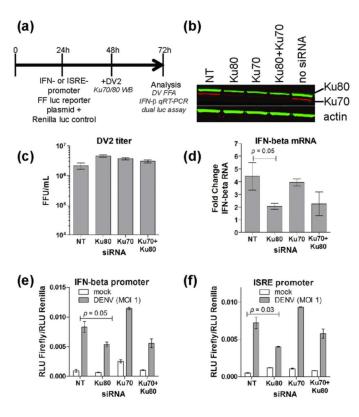
Figure 6. Partial Depletion of Ku80 by RNAi Is Associated with a Reduction in DV2-Induced Interferon-beta Expression and Signaling
(a) Schematic of the RNAi experiment. **(b)** Western blot analysis of steady-state Ku70 and Ku80 at 48 hours post-siRNA transfection confirming partial depletion of Ku70 and Ku80. Representative data for three independent experiments are shown. **(c)** DV2 titers at 24 hours post-infection were found to be unaffected by RNAi against Ku70 and/or Ku80 relative to the non-targeting (NT) control. **(d)** Partial depletion of Ku80 was associated with a modest but statistically significant decrease in IFN-beta mRNA ($p = 0.05$) as measured by qRT-PCR assay using IFN-beta-specific primers. Firefly luciferase expression driven by the **(e)** IFN-beta and **(f)** ISRE promoters was reduced at 48 hours post-DV2 infection in cells treated with Ku80-targeting siRNAs ($p = 0.05$ and 0.03, respectively) but not in cells treated with Ku70-targeting siRNAs or with the NT control. Firefly luciferase activity reflecting expression from the IFN-beta and ISRE reporters was normalized to the activity of the transfection control, renilla luciferase. Error bars represent the standard deviation of three independent experiments.